Journal of Zhejiang University-SCIENCE A (Applied Physics & Engineering)
ISSN 1673-565X (Print); ISSN 1862-1775 (Online)
www.zju.edu.cn/jzus; www.springerlink.com
E-mail: jzus@zju.edu.cn

Promoting the mechanical properties of Ti42Al9V0.3Y alloy by hot extrusion in the α+β phase region*

Wen-chen XU, Hao ZHANG, De-bin SHAN†‡

(*Department of Materials Science and Engineering, Harbin Institute of Technology, Harbin 150001, China*)

†E-mail: shandb@hit.edu.cn

Received Apr. 2, 2010; Revision accepted July 6, 2010; Crosschecked Aug. 31, 2010

Abstract: Hot extrusion was conducted in the α+β phase region for promoting mechanical properties of Ti42Al9V0.3Y. The microstructures and tensile properties before and after hot extrusion were studied. The results show that the microstructure of the as-cast alloy mainly consists of massive γ phase in β matrix and the as-extruded alloy mainly consists of lamellar α_2/γ, lamellar β/γ, and strip γ propagating from elongated β phase. In the as-cast alloy, the predominantly observed fracture mode is transgranular cleavage failure at room temperature and intergranular fracture at 650–750 °C. After hot extrusion, it transforms into transgranular cleavage-like failure, including translamellar cleavage and delamination. The excellent tensile properties of the as-extruded material are attributed to the obvious refined microstructure with broken YAl_2 particles and the micro-crack shielding action of the TiAl lamellasome.

Key words: TiAl alloy, Microstructure, Mechanical property, Hot extrusion
doi:10.1631/jzus.A1000138 **Document code:** A **CLC number:** TG113.25

1 Introduction

Owing to their low density, high specific strength, excellent oxidation and creep resistance at elevated temperatures, TiAl-based alloys are considered to be good candidates as high temperature structural materials for future hypersonic vehicles (Kestler and Clemens, 2003; Kim *et al.*, 2003; Das *et al.*, 2004). However, low ductility at room temperature and inferior workability at elevated temperatures restrict their application (Imayev *et al.*, 2007).

Tetsui *et al.* (2003; 2005) introduced β phase into TiAl-based alloys, and the industry forging practice proved that this type of TiAl-based alloy has excellent hot workability. But the mechanical property test indicated that the ambient ductility of the materials is still quite low (Tetsui *et al*., 2003). Chen *et al.* (2005) reported that the ductility of TiAl alloy can be improved by the addition of a small quantity of Y. Therefore, a TiAl-based alloy with nominal component Ti42Al9V0.3Y was developed, which consists of a lot of β phase and a small quantity of Y.

Tensile mechanical properties of TiAl alloys are sensitive to the microstructure. Particularly, the ambient ductility is improved by microstructural refinement (Liu and Maziasz, 1998; Park *et al.*, 1999; Chen *et al.*, 2002). Hot working is an efficient way to further refine the microstructure, which promote the ductility and other mechanical properties of TiAl alloy (Xu *et al.*, 2006). Thus, it is essential to study the effects of hot working on the microstructure and mechanical properties of TiAl alloy. In this study, the effects of hot extrusion on the microstructure and tensile properties of Ti42Al9V0.3Y alloy were investigated. Hot extrusion was conducted in the α+β phase region to achieve a good formability.

‡ Corresponding author

* Project supported by the National Postdoctoral Foundation of China, and the Youth Science and Technology Project of Harbin (No. 2008RFQXG040), China

2 Experimental

The alloy with nominal composition Ti42Al9V0.3Y (all in atomic percent, at.%) was prepared by induction skull melting (ISM). An ingot with dimensions of Φ120 mm×200 mm was prepared by casting into a steel mould. The composition was analyzed by the X-ray fluorescence method (Table 1). Then the ingot was hot isostatic pressed (HIP) under argon pressure to eliminate casting porosity (1250 °C, 175 MPa, 4 h).

Table 1 Composition of the alloy Ti42Al9V0.3Y

Element	Composition (at.%)
Ti	51.15
Al	41.49
V	9.40
Y	0.26

Cylindrical billets (Φ42 mm×35 mm) were cut from the ingot by electro-spark wire-electrode cutting, and then the billets were sealed in 5-mm thick stainless steel cases with ceramic sheets. After heating to 1325 °C with a holding time of 1 h, the samples were extruded in a single pass using a hydraulic press and the reduction in area was 1/9.

Tensile specimens with a gauge section of Φ3 mm×21 mm were prepared by low stress grinding and polishing with 1000 grit sand paper. All the specimens were taken from the extruded billet with the tensile direction parallel to the extrusion direction. Tensile tests in the temperature range from 20 to 750 °C were conducted on an Instron-5500R testing machine (Instron, USA) at an initial strain rate of 3.75×10^{-4} s^{-1}. The yield strength (S_Y), ultimate tensile strength (S_{UT}), and the plastic elongation to failure (δ) were determined by load-displacement curves from tensile tests.

Microstructures after extrusion were analyzed via scanning electron microscopy (SEM) in back-scattered electron (BSE) mode and transmission electron microscopy (TEM). Samples for TEM observation were prepared by twin-jet polishing. The electrolyte used for twin-jet polishing was a solution of 60% (v/v) methanol, 35% (v/v) butyl alcohol, and 5% (v/v) perchloric acid.

3 Results

3.1 Microstructures of the as-cast and as-extruded Ti42Al9V0.3Y alloy

The presence of γ and β phases (Fig. 1) was confirmed by X-ray diffraction (XRD) spectra of the alloy. As indicated from the SEM image in BSE mode (Fig. 2), the fine-grained black phase is surrounded by matrix phase with white contrast, and no lamellar structure is found in the as-cast Ti42Al9V0.3Y alloy. Energy dispersive X-ray spectroscopy (EDS) analysis reveals that the white phase contains a higher V element and the black phase contains a higher Al element than the nominal compositions of the alloy, so it can be concluded that the white phase is β phase and the black phase is γ phase. TEM and EDS analysis show that many particles with bright contrast are YAl_2 phase, mainly distributed in β matrix.

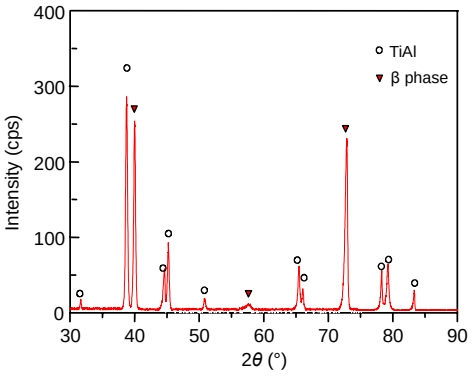

Fig. 1 X-ray diffraction pattern of Ti42Al9V0.3Y alloy

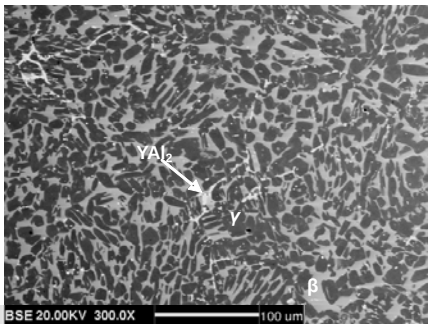

Fig. 2 Back-scattered electron microstructure of the as-cast Ti42Al9V0.3Y alloy

The phase with bright contrast is YAl_2, the phase with black contrast is γ, and the phase with white contrast is β

The SEM and TEM microstructures of Ti42Al9V0.3Y alloy after extrusion are shown in Fig. 3. The SEM image in BSE mode shows that the

as-extruded material has a complex microstructure (Fig. 3a). Figs. 3b and 3c are local amplifications of Fig. 3a. Fig. 3b shows two lamellar structures, one with grey contrast and the other one with black contrast. Figs. 3d and 3e exhibit the TEM microstructure with grey and black contrast in Fig. 3b, respectively. TEM diffraction analysis indicates that the grey lamellar structure consists of α_2/γ lamellae (Fig. 3d) and the black one consists of β/γ lamellae (Fig. 3e), but no fixed orientation relationship is observed between the β phase and γ phase. Fig. 3c shows the strip phase with black contrast precipitated from the band phase, with white contrast. Fig. 3f shows the TEM structure of the strip phase in Fig. 3c. TEM diffraction analysis confirms that the strip phase with white contrast is the γ phase and the band phase with black contrast is the β phase.

3.2 Tensile properties of the as-cast and as-extruded Ti42Al9V0.3Y alloy

Fig. 4 shows that the tensile mechanical properties of Ti42Al9V0.3Y alloy before and after extrusion have an obvious temperature dependence.

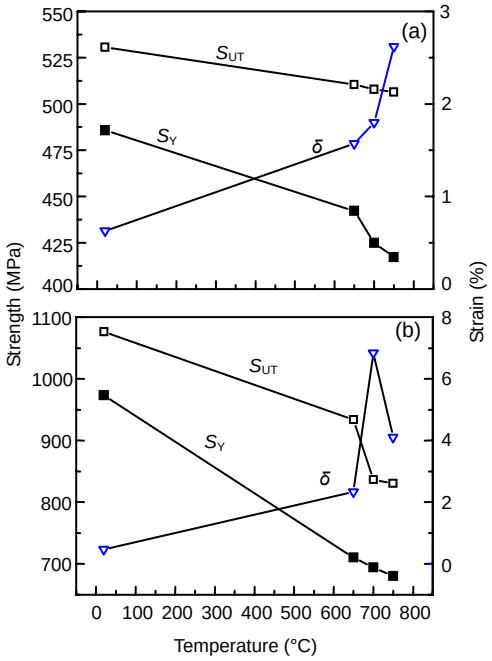

Fig. 4 Tensile properties of Ti42Al9V0.3Y alloy before and after extrusion

(a) As-cast alloy; (b) As-extruded alloy. The samples are obtained along the extrusion direction

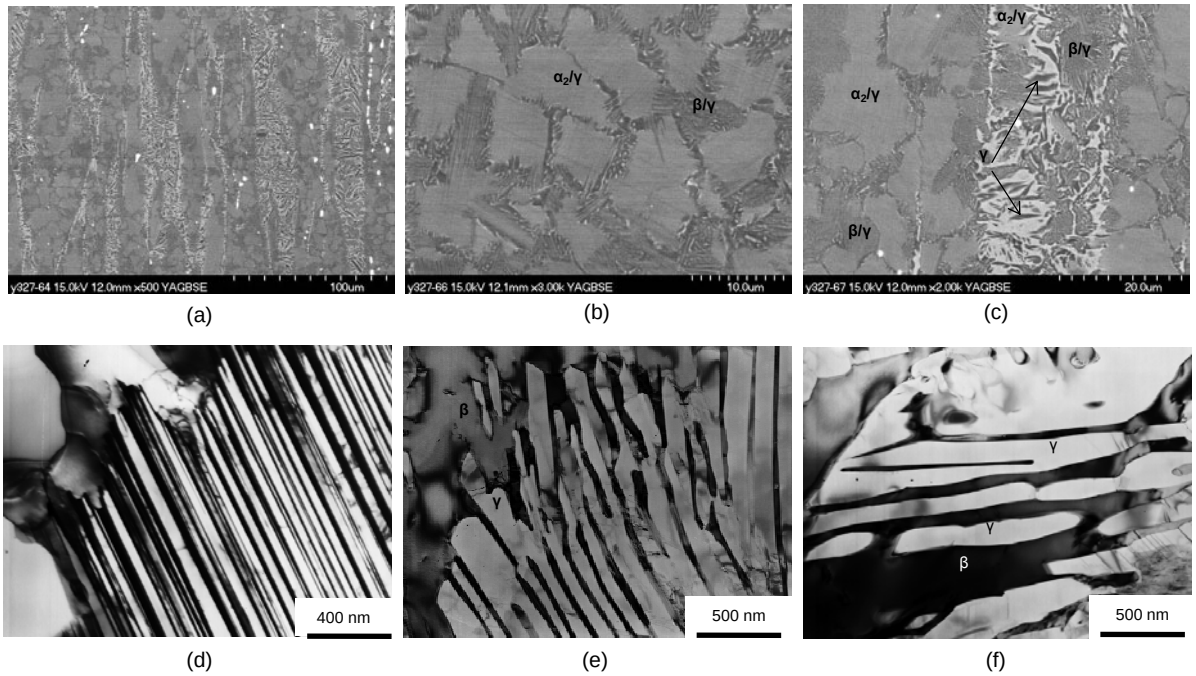

Fig. 3 SEM and TEM microstructures of Ti42Al9V0.3Y alloy after extrusion at 1325 °C

(a) SEM microstructure of as-extruded alloy; (b) SEM microstructure of two lamellar structures; (c) SEM microstructure of strip γ phase with black contrast precipitates from β phase with white contrast; (d) TEM microstructure of α_2/γ lamella (the white lamella is γ phase and the black one is α_2 lamella); (e) TEM microstructure of β/γ lamella (the white lamella is γ phase and the black one is β lamella); (f) TEM microstructure of strip γ phase (the white strip phase is γ phase and the black one is β phase). The extrusion direction is vertical, and the microstructures are observed on longitudinal section of the as-extruded bar

With the increase in temperature, S_Y and S_{UT} decrease and δ increases. It should be noted that, however, the ductility decreases suddenly at 750 °C in the as-extruded alloy, which may be caused by the oxidation of test samples. The S_{UT} of the material at room temperature is increased from 531 MPa (as-cast) to 1076 MPa (as-extruded). Respectively, the δ of the material at room temperature is increased from 0.628% to 1.47% with an enhancement of 134%. The S_{UT} of the material at 750 °C is increased from 507 MPa (as-cast) to 830 MPa (as-extruded). If the temperature at which δ rises to 7.5% is defined as the brittle-ductile transition temperature (TBD) (Xu *et al.*, 2006), the as-cast material has a TBD exceeding 750 °C, whereas the TBD value of the as-extruded material is less than 750 °C.

3.3 Fracture analysis for the as-cast and as-extruded Ti42Al9V0.3Y alloy

Figs. 5a and 5b show the fractographs of the as-cast Ti42Al9V0.3Y alloy at room temperature and 700 °C, respectively. At room temperature, the main fracture mechanism is transgranular cleavage fracture in β and γ phases with numerous cleavage planes. Fracture surfaces between long rod YAl_2 and β are observed in Fig. 5a, and they are approximately perpendicular to the tensile axis. The fracture mode of the as-cast material has an obvious temperature dependence, which becomes an intergranular fracture at 650–750 °C. The crack spreads along the phase interface between β and γ.

Figs. 5c and 5d show fractographs of the as-extruded material tested at room temperature and 700 °C. The fracture is dominated by transgranular cleavage-like failure, including translamellar cleavage and delamination.

4 Discussion

4.1 Effects of hot extrusion in α+β phase region on microstructure evolution

Fig. 6 presents the phase diagram of the vertical section in the Ti-Al-V ternary system at 42Al (at.%) which was reported by Tetsui *et al.* (2003). According to the phase diagram, the solidification and phase

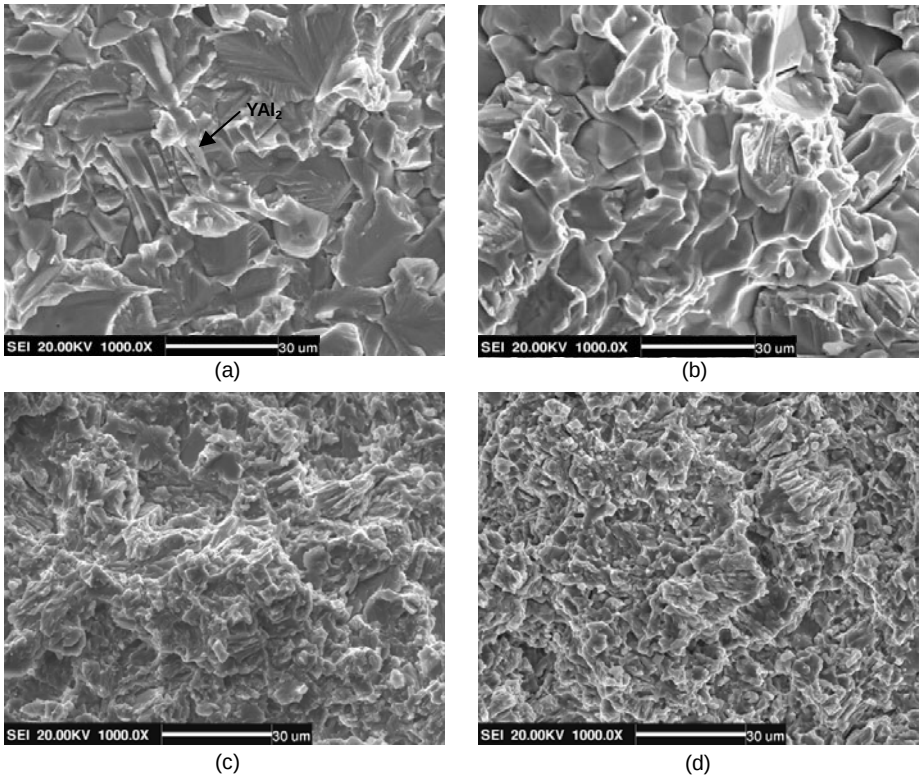

Fig. 5 Fractographs of the as-cast and as-extruded Ti42Al9V0.3Y alloy at room temperature and 700 °C
The tensile direction is parallel to the extrusion direction. (a) As-cast (room temperature); (b) As-cast (700 °C); (c) As-extruded (room temperature); (d) As-extruded (700 °C)

transformation path for the studied alloy is as follows: β→β+α→β+α+γ→β+α_2+γ→β+γ→B_2+γ. The as-cast Ti42Al9V0.3Y alloy has a quasi-equilibrium microstructure consisting of B_2 and γ after hot isostatic pression for 4 h at 1250 °C, followed by furnace cooling.

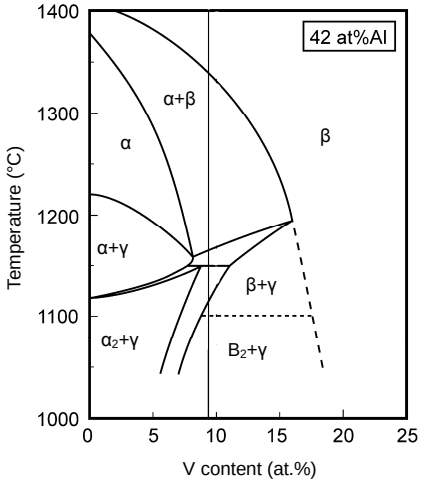

Fig. 6 Phase diagram of the vertical section in Ti-Al-V ternary system at 42Al (Tetsui *et al.*, 2003)

According to the differential scanning calorimetry (DSC) result, the phase transition β+α→β takes place at 1333 °C (T_β) in Ti42Al9V0.3Y alloy. Thus, the heating temperature (1325 °C) before hot extrusion is in the β+α phase region and the microstructure of the alloy consists of β grains rich in V and α grains poor in V. During hot extrusion, there is an obvious temperature rise surpassing the phase transition point T_β in the alloy due to a high extrusion velocity and a large extrusion ratio, which means that the hot extrusion process of Ti42Al9V0.3Y alloy is conducted in the β phase region. Owing to the high extrusion velocity in the β phase region, the alloy transforms into an elongated β phase with different element contents because of incomplete diffusion, one rich in V and the other poor in V. In the subsequent air cooling process, the phase transition of the elongated β microstructure poor in V should be as follows: β→β+α→lamellar (α/γ)+β→lamellar (α_2/γ)+lamellar (β/γ). At the same time, another phase transition process in the β phase rich in V should be β→β+γ. Thus, the final extrusion microstructure consists of two band microstructures with different contrast in BSE mode. The band microstructure with grey contrast (V-poor region) should include lamellar (α_2/γ) and lamellar (β/γ). And the black γ phase precipitates from the band microstructure with white contrast (V-rich region). The assertion of the phase transformation path is confirmed by Fig. 3.

4.2 Effects of microstructures on the tensile properties

The variation in the mechanical properties of Ti42Al9V0.3Y alloy before and after hot extrusion can be related to microstructure evolution during hot extrusion. The fracture analysis shows that the low bond strength in the interface between YAl_2 and β phase leads to crack initiation, and a low cleavage strength of β and γ phases contributes to crack propagation in the as-cast alloy (Fig. 3a). At 650–750 °C the inferior surface bond strength between β and γ leads to intergranular fracture (Fig. 3b). Therefore, the tensile strength and ductility are quite low in the as-cast alloy. The as-extruded alloy with fine lamellar structure shows better tensile properties than the as-cast alloy over the entire testing temperature range. It should be noted that the microstructure of the as-extruded material mainly consists of α_2/γ and β/γ lamellasome. The micro-crack generation in $\{111\}_\gamma$ of γ lamella is limited in adjacent α_2 lamella (Chan, 1993) or the interface between γ twin lamella (Appel and Wagner, 1998) and the micro plastic zone occurs at the tip of micro-crack. The micro-crack shielding action of the TiAl lamellasome improves the ductility and strength of the as-extruded alloy. At the same time, the microstructure refinement increases both the strength (Bohn *et al.*, 2001) and ductility (Senkov *et al.*, 1998) of the as-extruded alloy. As well, the long rod YAl_2 phase has been broken by hot extrusion, thus decreasing the fracture tendency caused by stress concentration in the as-extruded alloy.

5 Conclusions

The microstructure of as-cast alloy mainly consists of a massive γ phase in β matrix. After hot extrusion in the α+β phase region, the microstructure mainly consists of lamellar α_2/γ, lamellar β/γ, and a strip γ propagating from the elongated β phase. Lamellar α_2/γ and lamellar β/γ forms in an elongated β phase poor in V, and strip γ forms in an elongated β phase rich in V.

In the as-cast alloy, the predominantly observed fracture mode is a transgranular cleavage fracture at room temperature and intergranular fracture at 650–750 °C. In the as-extruded alloy, the fracture mode is a transgranular cleavage-like failure, including translamellar cleavage and delamination.

The mechanical property of Ti42Al9V0.3Y alloy can be greatly improved by hot extrusion in the α+β phase region. The low tensile properties of the as-cast alloy are attributed to the low cleavage strength of γ and β, weak surface bond strength between β and γ, and the existence of long rod YAl_2. The excellent tensile properties of the as-extruded alloy are attributed to the refined microstructure with broken YAl_2 particles and the micro-crack shielding action of the TiAl lamellasome.

References

Appel, F., Wagner, R., 1998. Microstructure and deformation of two-phase γ-titanium aluminides. *Material Science and Engineering: R: Reports*, **22**(5):258-259.

Bohn, R., Klassen, T., Bormann, R., 2001. Room temperature mechanical behavior of silicon-doped TiAl alloys with grain sizes in the nano- and submicron-range. *Acta Materialia*, **49**(2):299-311. [doi:10.1016/S1359-6454(00)00312-8]

Chan, K.S., 1993. Toughening mechanisms in titanium aluminides. *Metallurgical and Materials Transactions A*, **24**(3):569-583. [doi:10.1007/BF02656627]

Chen, Y.Y., Kong, F.T., Tian, J., Chen, Z.Y., Xiao, S.L., 2002. Recent developments in engineering γ-TiAl intermetallics. *Transactions of the Nonferrous Metals Society of China*, **12**(4):605-609.

Chen, Y.Y., Kong, F.T., Han, J.C., Chen, Z.Y., Tian, J., 2005. Influence of yttrium on microstructure, mechanical properties and deformability of Ti-43Al-9V alloy. *Intermetallics*, **13**(3-4):263-266.

Das, G., Kestler, H., Clemens, H., Bartolotta, P.A., 2004. Sheet gamma TiAl: status and opportunities. *JOM Journal of the Minerals, Metals and Materials Society*, **56**(11):42-45. [doi:10.1007/s11837-004-0251-y]

Imayev, R.M., Imayev, V.M., Oehring, M., Appel, F., 2007. Alloy design concepts for refined gamma titanium aluminide based alloys. *Intermetallics*, **15**(4):451-460. [doi:10.1016/j.intermet.2006.05.003]

Kestler, H., Clemens, H., 2003. Titanium and Titanium Alloys. Wiley-VCH, Weinheim, Germany.

Kim, Y.W., Clemens, H., Rosenberger, A.H., 2003. Gamma Titanium Aluminides. TMS, Warrendale, PA, USA.

Liu, C.T., Maziasz, P.J., 1998. Microstructural control and mechanical properties of dual-phase TiAl alloys. *Intermetallics*, **6**(7-8):653-661. [doi:10.1016/S0966-9795(98)00062-4]

Park, H.S., Nam, S.W., Kim, N.J., 1999. Refinement of the lamellar structure in TiAl-based intermetallic compound by addition of carbon. *Scripta Materialia*, **41**(11):1197-1203. [doi:10.1016/S1359-6462(99)00266-3]

Senkov, O.N., Srisukhumbowornchai, N., Ovecoglu, M.L., Froes, F.H., 1998. Microstructure evolution of a nanocrystalline Ti-47Al-3Cr alloy on annealing at 1200 °C. *Scripta Materialia*, **39**(6):691-698. [doi:10.1016/S1359-6462(98)00233-4]

Tetsui, T., Shindo, K., Kaji, S., Kobayashi, S., Takeyama, M., 2003. Strengthening a high-strength TiAl alloy by hot-forging. *Intermetallics*, **11**(4):299-306. [doi:10.1016/S0966-9795(02)00245-5]

Tetsui, T., Shindo, K., Kaji, S., Kobayashi, S., Takeyama, M., 2005. Fabrication of TiAl components by means of hot forging and machining. *Intermetallics*, **13**(9):971-978. [doi:10.1016/j.intermet.2004.12.012]

Xu, X.J., Lin, J.P., Wang, Y.L., Gao, J.F., Lin, Z., Chen, G.L., 2006. Effect of forging on microstructure and tensile properties of Ti-45Al-(8–9)Nb-(W,B,Y) alloy. *Journal of Alloys and Compounds*, **414**(1-2):175-180. [doi:10.1016/j.jallcom. 2005.03.121]

2009 JCR of Thomson Reuters for *JZUS-A* and *JZUS-B*

ISI Web of Knowledge℠

Journal Citation Reports®

WELCOME | HELP | RETURN TO LIST | PREVIOUS JOURNAL | NEXT JOURNAL

2009 JCR Science Edition

Journal: Journal of Zhejiang University-SCIENCE A

Mark	Journal Title	ISSN	Total Cites	Impact Factor	5-Year Impact Factor	Immediacy Index	Citable Items	Cited Half-life	Citing Half-life
☐	J ZHEJIANG UNIV-SC A	1673-565X	322	0.301		0.066	213	3.0	6.8

Journal: Journal of Zhejiang University-SCIENCE B

Mark	Journal Title	ISSN	Total Cites	Impact Factor	5-Year Impact Factor	Immediacy Index	Citable Items	Cited Half-life	Citing Half-life
☐	J ZHEJIANG UNIV-SC B	1673-1581	619	1.041		0.156	128	3.1	7.5